

Cross Polarization for Dissolution Dynamic Nuclear Polarization Experiments at Readily Accessible Temperatures $1.2 < T < 4.2$ K

Aurélien Bornet · Roberto Melzi · Sami Jannin ·
Geoffrey Bodenhausen

Received: 20 March 2012 / Revised: 8 May 2012 / Published online: 6 June 2012
© Springer-Verlag 2012

Abstract Cross polarization can provide significant enhancements with respect to direct polarization of low- γ nuclei such as ^{13}C . Substantial gains in sample throughput (shorter polarization times) can be achieved by exploiting shorter build-up times $\tau_{\text{DNP}}(^1\text{H}) < \tau_{\text{DNP}}(^{13}\text{C})$. To polarize protons rather than low- γ nuclei, nitroxide radicals with broad ESR resonances such as TEMPO are more appropriate than Trityl and similar carbon-based radicals that have narrow lines. With TEMPO as polarizing agent, the main Dynamic Nuclear Polarization (DNP) mechanism is thermal mixing (TM). Cross polarization makes it possible to attain higher polarization levels at 2.2 K than one can obtain with direct DNP of low- γ nuclei with TEMPO at 1.2 K, thus avoiding complex cryogenic technology.

A. Bornet · S. Jannin (✉) · G. Bodenhausen
Institut des Sciences et Ingénierie Chimiques, Ecole Polytechnique Fédérale
de Lausanne (EPFL), Batochime, 1015 Lausanne, Switzerland
e-mail: sami.jannin@gmail.com

R. Melzi
Bruker Italia S.r.l, Viale V. Lancetti, 43, 20158 Milan, Italy

G. Bodenhausen
Département de Chimie, Ecole Normale Supérieure, 24 Rue Lhomond,
75231 Paris Cedex 05, France

G. Bodenhausen
Université Pierre-et-Marie Curie, Paris, France

G. Bodenhausen
UMR 7203, CNRS/UPMC/ENS, Paris, France

1 Introduction

Dissolution Dynamic Nuclear Polarization (DNP) [1] is generally carried out at low temperatures ($1.2 < T < 1.5$ K) where nuclear spins $S = 1/2$ with low gyromagnetic ratios γ_S (^{13}C , ^{15}N [2], ^{129}Xe [3], ^{89}Y [4], etc.) are polarized directly by microwave irradiation that saturates the EPR transitions of stable radicals such as TEMPO or Trityl. This is followed by rapid dissolution [5] and transport to a solution-state NMR or MRI system. This technique can yield enhancements of NMR signals on the order of $\varepsilon = 10,000$ with respect to the Boltzmann polarization at room temperature, provided that the highly polarized nuclear spins retain most of their polarization during dissolution and transfer.

Nuclear spins with high gyromagnetic ratios γ_I such as ^1H and ^{19}F tend to return rapidly to thermal equilibrium, so that, by the time the samples have arrived in the solution-state NMR or MRI system, the remaining enhancements are modest [6]. Moreover, it is often not feasible to follow a chemical reaction or a metabolic process on the short T_1 time scale of spins with high gyromagnetic ratios. Recently, several techniques have been developed to extend their lifetimes beyond T_1 [7–9]. Nevertheless, nuclear spins S with low gyromagnetic ratios γ_S such as ^{13}C or ^{15}N are much preferred in most dissolution DNP experiments.

It has been demonstrated that Trityl radicals can be very efficient as polarizing agents for ^{13}C . These carbon-centered radicals feature ESR lines with narrow widths $\Delta\nu_e$, thus facilitating the direct build-up of ^{13}C polarization by thermal mixing since $\Delta\nu_e > \nu_0(^{13}\text{C})$, while leaving the ^1H spins close to their thermal equilibrium since $\Delta\nu_e < \nu_0(^1\text{H})$. The highest ^{13}C polarization reported so far [10] (without cross polarization) in a field $B_0 = 3.35$ T is $P^{\text{DNP}}(^{13}\text{C}) = (P_\alpha - P_\beta)/(P_\alpha + P_\beta) = 35$ % with a build-up time constant $\tau_{\text{DNP}}(^{13}\text{C}) = 2300$ s at $T = 1$ K. Although such high polarization levels can provide intense NMR signals after dissolution, the long DNP build-up times $\tau_{\text{DNP}}(^{13}\text{C})$ do not allow one to perform several dissolution processes in rapid succession, as required for many in vivo experiments with high throughput. Two approaches have been described recently to enable multiple in vivo experiments at higher repetition rates: the design of a multiple-sample DNP polarizer [11] and the use of cross polarization [12–14].

While the design of a sample changer at very low temperatures is a challenge, the implementation of cross polarization (CP) appears more straightforward. Until recently, CP did not raise much interest, for a significant part of the dissolution DNP community focused on the use of Trityl radicals that are efficient for spins with low gyromagnetic ratios γ like ^{13}C , ^{15}N , ^{129}Xe , ^{89}Y , etc., but not for protons. This is not true for DNP combined with MAS (usually around $T = 100$ K) where the dominant DNP mechanism for nitroxide biradicals is usually the cross effect, and where CP schemes have been successfully applied [15].

On the other hand, for those who prefer to avoid Trityl radicals for ^{13}C DNP (possibly for economic reasons), the inexpensive radical (2, 2, 6, 6-tetramethylpiperidin-1-yl)oxyl (TEMPO) turns out to be a good option. Admittedly, the polarization levels that have been quickly achieved with TEMPO, typically $P^{\text{DNP}}(^{13}\text{C}) = 10$ % with $\tau_{\text{DNP}}(^{13}\text{C}) \approx 600$ s in a field $B_0 = 3.35$ T at $T = 1.5$ K [16, 17], are modest compared to those achieved with Trityl. TEMPO has a broad

inhomogeneous ESR line, mainly broadened by g -anisotropy, and its line-width at 1.2 K can exceed the ^1H Larmor frequency $\nu_0(^1\text{H}) = 142.7$ MHz at 3.35 T. These properties allow one to fulfill the conditions for ^1H DNP to occur preferably via thermal mixing (TM). One of the main consequences of TM, predicted theoretically [18] and observed experimentally [17], is that all nuclear spins with spin $S = 1/2$ in the sample acquire a common spin temperature T_S and a polarization P that is determined by their Larmor frequency:

$$P = \tanh\left(\frac{\hbar\omega}{2k_B T_S}\right)$$

Thermal contact with the ^1H spins inevitably results in an enhancement not only of the polarization $P(^{13}\text{C})$ but also of $P(^1\text{H})$, albeit at the price of a higher (less favorable) spin temperature T_S because of the ‘heat load’ of the ^1H spin bath.

2 ESR Features of the Polarizing Agent

Excessively wide ESR lines are detrimental to the efficiency of DNP via TM. This effect has been thoroughly described by Provotorov [19] in the high temperature approximation and by Borghini [20] for low temperatures, and experimental results have been published by Heckmann and co-workers [21]. If the ESR lines are too wide, nuclear spins I with high γ_I , tend to become involved in the DNP process when TM is dominant. Nuclear spins with high γ acquire an enhanced polarization, in part at the expense of the polarization of spins S with low γ_S . A ‘leakage factor’ was introduced in the Borghini theory by De Boer [22] to account for this phenomenon, which can simply be described by a loss of polarization via spin–lattice relaxation of the I spins. The importance of this leakage for the polarization of the S spins (such as ^{13}C) is illustrated in Fig. 1. For 3 M ^{13}C -labeled sodium acetate (CH_3COONa) samples dissolved with 30 mM TEMPO in 2:1 v/v

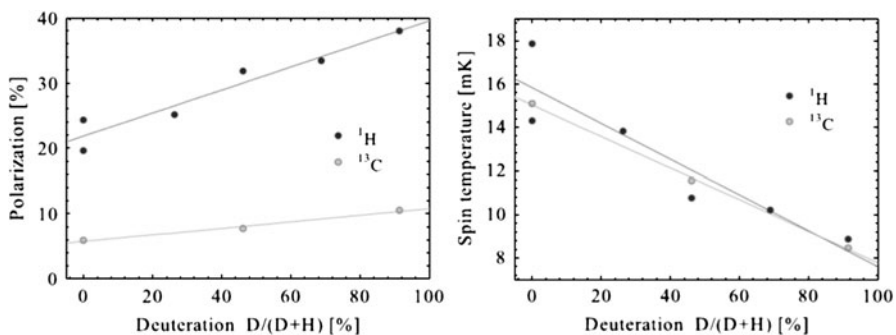


Fig. 1 The proton and carbon-13 polarizations and the spin temperature in 3 M ^{13}C -labeled sodium acetate with 30 mM TEMPO in a partly deuterated water:ethanol (2:1 v/v) mixtures at 1.2 K and 3.5T under 35 mW microwave irradiation at 97.2 GHz suffer from leakage depending on the level of deuteriation of the solvent. Adapted with permission from Ref. [17]

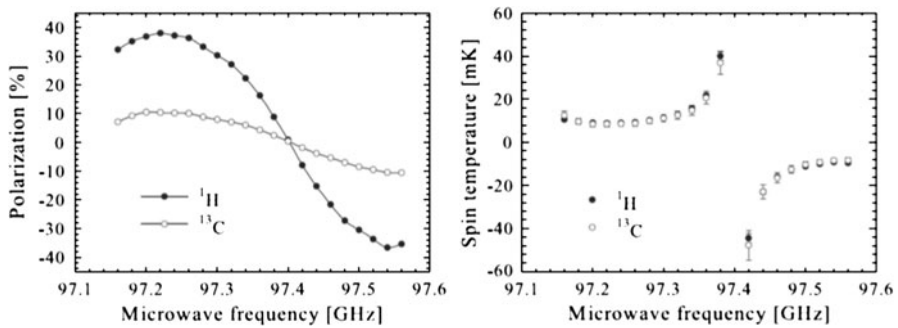


Fig. 2 Carbon and proton spin polarizations and spin temperature in 3 M ^{13}C -labeled sodium acetate with 30 mM TEMPO in a partly deuterated water:ethanol (2:1 v/v) mixture at 1.2 K and 3.5T under 35 mW microwave irradiation near 97.2 GHz as a function of the offset of the microwave frequency with respect to the center of the ESR line of TEMPO. Adapted with permission from Ref. [17]

water:ethanol mixtures that are partly deuterated (water and ethanol being deuterated in the same proportion) (see Fig. 1), the enhancement of the ^{13}C polarization strongly depends on the deuteration of the solvent. The rate of the leakage of spins I and/or S increases with the square of the gyromagnetic ratio γ_I ; hence spins S with low γ_S only play a minor role that could not be determined quantitatively.

3 Sample Properties for Cross Polarization Combined with Dynamic Nuclear Polarization (CP-DNP)

Since DNP with TEMPO takes place via TM, an uniform spin temperature T_S is established after a certain time. Once the ‘DNP equilibrium’ is reached, the polarizations $P^{\text{DNP}}(I)$ and $P^{\text{DNP}}(S)$ of different nuclear spin species I and S in the samples are simply proportional to their gyromagnetic ratios. Thus proton spins display the highest spin polarization among all nuclear spins except tritium. Figure 2 shows how both ^{13}C and ^1H end up with identical spin temperatures T_S and polarizations $P^{\text{DNP}}(^1\text{H})/P^{\text{DNP}}(^{13}\text{C}) = \gamma(^1\text{H})/\gamma(^{13}\text{C}) \approx 4$ regardless of the microwave frequency. Figure 3 presents DNP build-up curves for both ^{13}C and ^1H . The DNP build-up time $\tau_{\text{DNP}}(^1\text{H}) = 70$ s is shorter than $\tau_{\text{DNP}}(^{13}\text{C}) = 324$ s by a factor $\kappa = 4.6$. These two facts provide ample evidence of the utility of CP for DNP experiments when TM is the dominant mechanism, as occurs with TEMPO. As explained above, one has to carefully choose the degree of deuteration of the solvent in order to achieve efficient CP without significantly sacrificing the DNP enhancement. In many molecules, the presence of covalently attached protons in the neighborhood of the ^{13}C nuclei (separated by only two bonds for $^{13}\text{C}=\text{O}$ in acetate) turns out to be sufficient for CP to be efficient. In this study, we therefore chose 3 M solutions of ^{13}C enriched sodium acetate with 30 mM TEMPO dissolved in a fully deuterated water:ethanol (2:1 v/v) mixture.

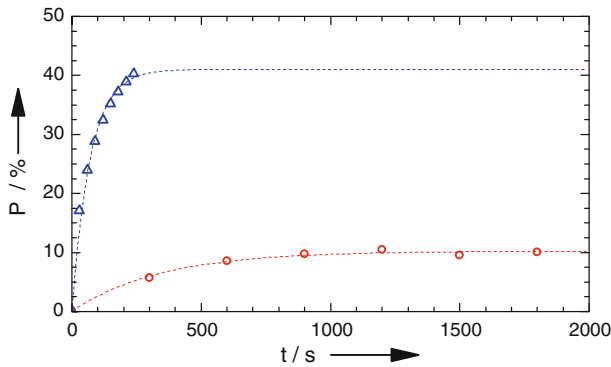


Fig. 3 Build-up behavior of carbon-13 (*squares*) and proton (*triangles*) polarization in 3 M ^{13}C -labeled sodium acetate with 30 mM TEMPO in a 100 % deuterated water:ethanol (2:1 v/v) mixture at 1.2 K and 3.35 T with 35 mW microwave irradiation at 93.9 GHz

4 Methods for Dynamic Nuclear Polarization (DNP)

Our home-built polarizer [16] operates at 3.35 T in the temperature range $1.2 < T < 4.2$ K, with a tunable microwave source (ELVA) operating in CW mode in the power range $1.5 < P_{\mu\text{w}} < 225$ mW. Apart from $T = 1.2$ K, where a maximum DNP could be achieved with $P_{\mu\text{w}} = 35$ mW, the maximum available power $P_{\mu\text{w}} = 225$ mW was used for all other experiments. The NMR signals were observed with a solid-state NMR spectrometer coupled to a home-built doubly tuned probe providing radio frequency field (*rf*) amplitudes up to $\gamma B_1 / (2\pi) = 50$ kHz for both spins *I* and *S* (142.6 MHz for ^1H and 35.87 MHz for ^{13}C at 3.35T) with a moderate *rf* power $P_{\text{rf}} = 25$ W on both channels [13].

5 DNP Results

Table 1 shows the polarization levels $P(^{13}\text{C})$ and $P(^1\text{H})$ and build-up times $\tau_{\text{DNP}}(^{13}\text{C})$ and $\tau_{\text{DNP}}(^1\text{H})$ obtained at different temperatures, with and without CP. Figure 4 shows how the maximum polarization levels obtained at different temperatures are roughly inversely proportional to the sample temperature for both

Table 1 Polarizations $P^{\text{DNP}}(^{13}\text{C})$ and $P^{\text{DNP}}(^1\text{H})$ and corresponding build-up times $\tau_{\text{DNP}}(^{13}\text{C})$ and $\tau_{\text{DNP}}(^1\text{H})$ determined in 3 M ^{13}C -labeled sodium acetate with 30 mM TEMPO in a 100 % deuterated water:ethanol (2:1 v/v) mixture at $T = 1.2, 2.2, 3.0$ and 4.2 K

T (K)	$P^{\text{DNP}}(^{13}\text{C})$ (%)	$\tau_{\text{DNP}}(^{13}\text{C})$ (s)	$P^{\text{DNP}}(^1\text{H})$ (%)	$\tau_{\text{DNP}}(^1\text{H})$ (s)
1.2	10	324	40	70
2.2	6	267	24	57
3	3	222	12	32
4.2	2	158	8	22

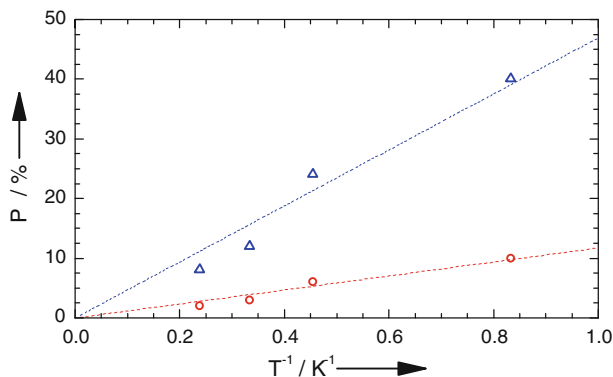


Fig. 4 Polarizations of carbon-13 (squares) and protons (triangles) in 3 M ^{13}C -labeled sodium acetate with 30 mM TEMPO in a 100 % deuterated water:ethanol (2:1 v/v) mixture obtained without CP at temperatures $T = 1.2, 2.2, 3,$ and 4.2 K plotted as a function of the inverse temperature $1/T$. The dashed lines are fits with $P = a/T$ with $a = 11.7$ K for carbon-13 and $a = 46.9$ K for protons

^{13}C and ^1H , as expected from spin temperature considerations [19, 20]. Thus, the proton polarization $P^{\text{DNP}}(^1\text{H}, 4.2 \text{ K}) = 8 \%$ at a comparatively high sample temperature of 4.2 K is nearly as high the carbon-13 polarization $P^{\text{DNP}}(^{13}\text{C}, 1.2 \text{ K}) = 10 \%$ at 1.2 K.

As the temperature is increased, electron spin–lattice relaxation times become shorter, regardless of whether electron relaxation is dominated by direct or by two-phonon Raman processes. As a result, higher microwave intensities are needed to saturate the ESR line at higher temperatures since:

$$I = \frac{I_0}{1 + \gamma^2 B_1^2 T_1 g(\omega)}$$

Figure 5 shows ^{13}C polarizations obtained for different temperatures and microwave power levels $P_{\mu\text{w}}$. Saturation can easily be achieved at $T = 1.2$ K with a modest microwave power ($P_{\mu\text{w}} \approx 30$ mW), but more power is required at higher temperatures. Although the build-up times (Fig. 5b) do not depend significantly on microwave power, they are dramatically accelerated at higher temperatures. The ^1H polarization build-up time is boosted by a factor $\kappa(^1\text{H}) = R_{\text{DNP}}(4.2 \text{ K})/R_{\text{DNP}}(1.2 \text{ K}) = \tau_{\text{DNP}}(1.2 \text{ K})/\tau_{\text{DNP}}(4.2 \text{ K}) = 3.2$.

6 Cross Polarization Combined with Dynamic Nuclear Polarization (CP-DNP)

In the regime of thermal mixing that dominates if one uses TEMPO, CP allows one to boost the polarization from $P^{\text{DNP}}(^{13}\text{C})$ to $P^{\text{CP-DNP}}(^1\text{H} \rightarrow ^{13}\text{C}) \approx P^{\text{DNP}}(^1\text{H})$. The use of CP makes it possible for example to obtain better performance at 2.2 K as direct ^{13}C DNP without CP at 1.2 K, thus allowing the cryogenic equipment to be greatly simplified. Another advantage of CP is the acceleration of the experiments by a factor $\kappa_{\text{CP}} = R_{\text{DNP}}(^1\text{H})/R_{\text{DNP}}(^{13}\text{C}) = \tau_{\text{DNP}}(^{13}\text{C})/\tau_{\text{DNP}}(^1\text{H})$. Table 2 and Fig. 6 show polarization levels $P^{\text{CP-DNP}}(^1\text{H} \rightarrow ^{13}\text{C})$ and $P^{\text{DNP}}(^{13}\text{C})$ that can be compared

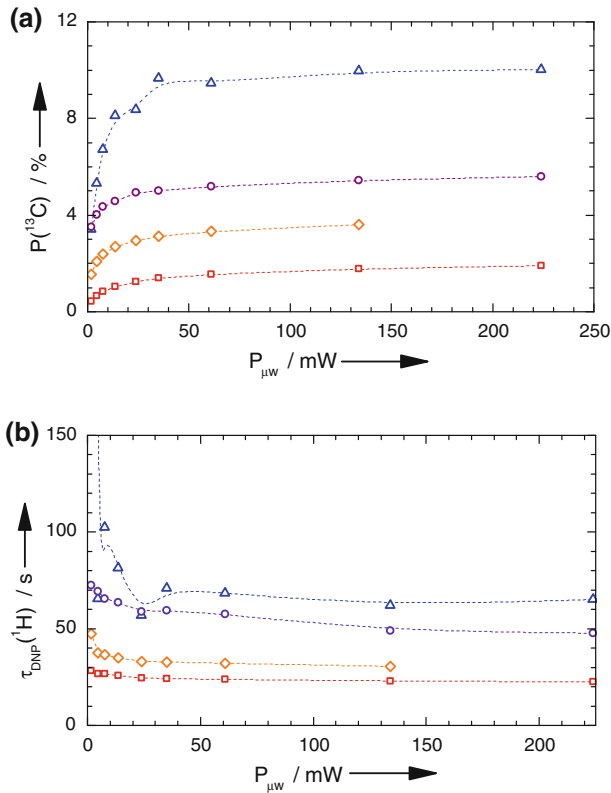


Fig. 5 (a) ^{13}C polarization in 3 M ^{13}C -labeled sodium acetate with 30 mM TEMPO in a 100 % deuterated water:ethanol (2:1 v/v) mixture as a function of the microwave power at 93.9 GHz and 3.35 T for $T = 1.2$ (triangles), 2.2 (circles), 3.0 (diamonds), and 4.2 (squares) K. (b) Build-up times $\tau_{\text{DNP}}(^1\text{H})$ at the same temperatures

with those presented in Table 1. In practice, with our instrumentation, CP provides an approximately twofold enhancement compared to conventional direct DNP. Further improvement in coil design (better B_1 homogeneity and less arching), faster switching of the rf phase and power (currently about 4 μs) may allow us to further boost the enhancement factors.

The CP efficiency strongly depends on the amplitudes of the rf fields, which should ideally be larger than the NMR linewidths. In static samples at low temperatures, the main limitation arises from the breadth of the ^1H spectrum, which is typically on the order of 50 kHz. Figure 7 shows the CP efficiency as a function of the rf amplitude B_1 for conventional CP, which suggests that a higher CP efficiency could be attained with higher B_1 , provided the probe can be made less prone to arching. More elaborate CP schemes employing frequency swept pulses could be used [14] to improve the CP efficiency despite the limited rf amplitudes.

Table 2 ^{13}C polarization in 3 M ^{13}C -labeled sodium acetate with 30 mM TEMPO in a 100 % deuterated water:ethanol (2:1 v/v) mixture obtained after CP achieved at 3.35 T in the range $1.2 < T < 4.2$ K

T (K)	$P^{\text{CP}}(^1\text{H} \rightarrow ^{13}\text{C})$ (%)	ε_{CP}	κ
1.2	19	1.9	4.6
2.2	14.6	2.4	4.7
3	7.2	2.4	6.9
4.2	4.4	2.2	7.2

The enhancement ε_{CP} is defined as the ^{13}C signal obtained after cross polarization normalized by the signal obtained by direct excitation

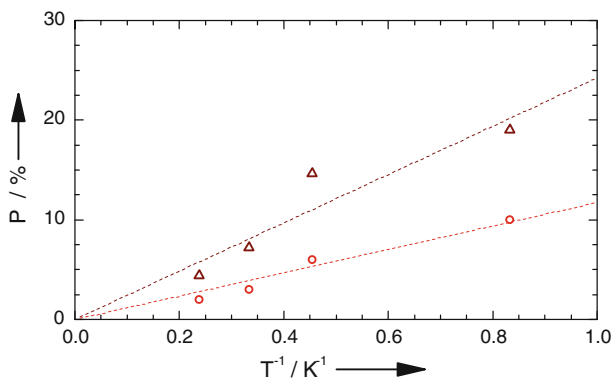


Fig. 6 Polarization levels $P^{\text{CP-DNP}}(^1\text{H} \rightarrow ^{13}\text{C})$ and $P^{\text{DNP}}(^{13}\text{C})$ in 3 M ^{13}C -labeled sodium acetate with 30 mM TEMPO in a 100 % deuterated water:ethanol (2:1 v/v) mixture obtained with (triangles) and without (circles) CP at 3.35T for temperatures $T = 1.2, 2.2, 3,$ and 4.2 K plotted as a function of the inverse temperature $1/T$. The dashed lines represent linear fits with $P = a/T$ with $a = 24.3$ K and 11.7 K for carbon-13 with (triangles) and without (circles), respectively

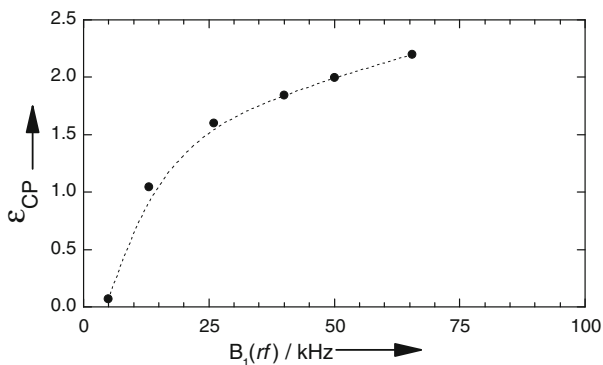


Fig. 7 The enhancement ε_{CP} as a function of the rf amplitude B_1 applied to both nuclei I and S (in this case ^1H and ^{13}C) in 3 M ^{13}C -labeled sodium acetate with 30 mM TEMPO in a 100 % deuterated water:ethanol (2:1 v/v) mixture

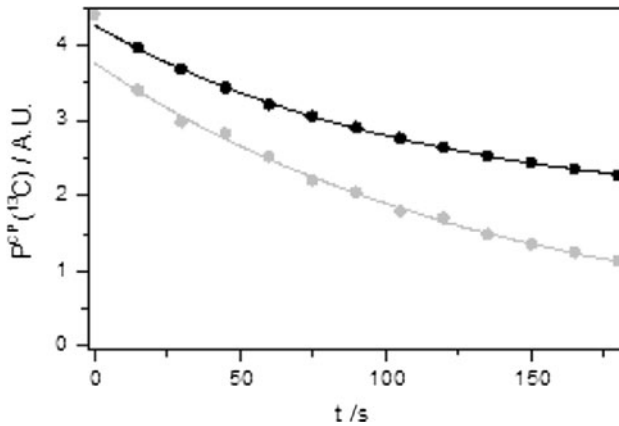


Fig. 8 Longitudinal ^{13}C relaxation in 3 M ^{13}C -labeled sodium acetate with 30 mM TEMPO in a 100 % deuterated water:ethanol (2:1 v/v) mixture after CP at 4.2 K and 3.35 T, either with 93.9 GHz microwave irradiation 'on' continuously (black dots) or switched 'off' after CP (gray dots)

7 Relaxation after CP

In view of performing rapid dissolution to produce hyperpolarized samples for solution-state NMR, we studied the relaxation behavior of the highly polarized ^{13}C spins immediately after CP (Fig. 8). If the microwave field remains 'on', the polarization $P^{\text{CP-DNP}}(^1\text{H} \rightarrow ^{13}\text{C})$ returns to the stationary state $P^{\text{DNP}}(^{13}\text{C})$. We do not intend to give a detailed analysis of the time constant of this process, but it is worth stressing the fact that it is much shorter than $T_1(^{13}\text{C})$, and close to $\tau_{\text{DNP}}(^{13}\text{C})$. This behavior can be explained by the fact that DNP occurs via TM. The result is even more intriguing when microwaves are switched 'off' after CP, since in this case the protons also start to relax, so that the return of $P^{\text{CP-DNP}}(^1\text{H} \rightarrow ^{13}\text{C})$ to thermal equilibrium will depend on $T_1(^1\text{H})$, $T_1(^{13}\text{C})$ and $\tau_{\text{DNP}}(^{13}\text{C})$. However, all these time constants are sufficiently long (>100 s even at 4.2 K) to allow one to perform rapid dissolution within a few seconds after CP.

8 Conclusions

Cross polarization is a method of choice for dissolution DNP experiments. It provides significant enhancements with respect to direct polarization of low- γ nuclei such as ^{13}C , and substantial gains in build-up times. If one uses the radical TEMPO as polarizing agent, the main DNP mechanism is thermal mixing, and the lifetime of CP-enhanced ^{13}C polarization is sufficiently long to allow one to carry out dissolution experiments. Compared to direct polarization of low- γ nuclei, cross polarization provides a means of reaching higher polarization levels at a given temperature. The use of CP makes it possible to attain higher polarization levels at 2.2 K with TEMPO than one can obtain with direct DNP at 1.2 K, thus avoiding complex cryogenic technology.

Acknowledgments The authors thank Dr. Jacques van der Klink for theoretical insights and Martial Rey for valuable technical assistance. This work was supported by the Swiss National Science Foundation, the Ecole Polytechnique Fédérale de Lausanne (EPFL), the Swiss Commission for Technology and Innovation (CTI), and the French CNRS.

References

1. A. Abragam, M. Goldman, Principles of dynamic nuclear polarization. Reports on Progress in Physics **2**, **41**(3), 395–467 (1978)
2. R. Sarkar, A. Comment, P.R. Vasos, S. Jannin, R. Gruetter, G. Bodenhausen, H. Hall, D. Kirik, V.P. Denisov, Proton NMR of ^{15}N choline metabolites enhanced by dynamic nuclear polarization. J. Am. Chem. Soc. **131**(44), 16014–16015 (2009)
3. A. Comment, S. Jannin, J.N. Hyacinthe, P. Miéville, R. Sarkar, P. Ahuja, P.R. Vasos, X. Montet, F. Lazeyras, J.P. Vallée, P. Hautle, J.A. Konter, B. van den Brandt, J.P. Ansermet, R. Gruetter, G. Bodenhausen, Hyperpolarizing gases via dynamic nuclear polarization and sublimation. Phys. Rev. Lett. **105**(1), 018104 (2010)
4. P. Miéville, S. Jannin, L. Helm, G. Bodenhausen, Kinetics of yttrium-ligand complexation monitored using hyperpolarized ^{89}Y as a model for gadolinium in contrast agents. J. Am. Chem. Soc. **132**(14), 5006–5007 (2010)
5. J.H. Ardenkjaer-Larsen, B. Fridlund, A. Gram, G. Hansson, L. Hansson, M.H. Lerche, R. Servin, M. Thaning, K. Golman, Increase in signal-to-noise ratio of $>10,000$ times in liquid-state NMR. Proc. Natl. Acad. Sci. USA **100**(18), 10158–10163 (2003)
6. P. Miéville, S. Jannin, G. Bodenhausen, Relaxometry of insensitive nuclei: optimizing dissolution dynamic nuclear polarization. J. Magn. Reson. **210**(1), 137–140 (2011)
7. M. Caravetta, O.G. Johannessen, M.H. Levitt, Beyond the T_1 limit: singlet nuclear spin states in low magnetic fields. Phys. Rev. Lett. **92**(15), 153003–153007 (2004)
8. P. Ahuja, R. Sarkar, S. Jannin, P.R. Vasos, G. Bodenhausen, Proton hyperpolarisation preserved in long-lived states. Chem. Comm. **46**(43), 8192–8194 (2010)
9. P.R. Vasos, A. Comment, R. Sarkar, P. Ahuja, S. Jannin, J.P. Ansermet, J.A. Konter, P. Hautle, B. van den Brandt, G. Bodenhausen, Long-lived states to sustain hyperpolarized magnetization. Proc. Natl. Acad. Sci. USA **106**(44), 18475–18479 (2009)
10. J.H. Ardenkjaer-Larsen, A.M. Leach, N. Clarke, J. Urbahn, D. Anderson, T.W. Skloss, Dynamic nuclear polarization polarizer for sterile use intent. NMR Biomed. **24**(8), 927–932 (2011)
11. M. Batel, M. Krajewski, K. Weiss, O. With, A. Däpp, A. Hunkeler, M. Gimersky, K.P. Pruessmann, P. Boesiger, B.H. Meier, S. Kozerke, M. Ernst, A multi-sample 94 GHz dissolution dynamic-nuclear-polarization system. J. Magn. Reson. **214**, 166–174 (2012)
12. S.R. Hartmann, E.L. Hahn, Nuclear double resonance in the rotating frame. Phys. Rev. **128**(5), 2042 (1962)
13. S. Jannin, A. Bornet, S. Colombo, G. Bodenhausen, Low-temperature cross-polarization in view of enhancing dissolution dynamic nuclear polarization in NMR. Chem. Phys. Lett. **517**(4–6), 234–236 (2011)
14. A.J. Pérez Linde, *Application of cross polarisation techniques to dynamic nuclear polarisation dissolution experiments*. School of Physics and Astronomy, University of Nottingham, Nottingham (2010)
15. D.A. Hall, D.C. Maus, G.J. Gerfen, S.J. Inati, L.R. Becerra, F.W. Dahlquist, R.G. Griffin, Polarization-enhanced NMR spectroscopy of biomolecules in frozen solution. Science **276**(5314), 930–932 (1997)
16. A. Comment, B. van den Brandt, K. Uffmann, F. Kurdzesau, S. Jannin, J.A. Konter, P. Hautle, W.T.H. Wenckebach, R. Gruetter, J.J. van der Klink, Design and performance of a DNP prepolarizer coupled to a rodent MRI scanner. Concepts Magn. Reson. B **31B**(4), 255–269 (2007)
17. F. Kurdzesau, B. van den Brandt, A. Comment, P. Hautle, S. Jannin, J.J. van der Klink, J.A. Konter, Dynamic nuclear polarization of small labelled molecules in frozen water–alcohol solutions. J. Phys. D **41**(15), 155506 (2008)
18. A. Abragam, M. Goldman, Principles of dynamic nuclear-polarization. Rep. Prog. Phys. **41**(3), 395–467 (1978)
19. M.A. Kozhushner, B.N. Provotorov, On the theory of dynamic nuclear polarization in crystals. Sov. Phys. Sol. State **6**(5), 1152–1154 (1964)

20. M. Borghini, Spin-temperature model of nuclear dynamic polarization using free radicals. *Phys. Rev. Lett.* **20**(9), 419 (1968)
21. J. Heckmann, W. Meyer, E. Radtke, G. Reicherz, Electron spin resonance and its implication on the maximum nuclear polarization of deuterated solid target materials. *Phys. Rev. B* **74**(13), 134418 (2006)
22. W. Boer, M. Borghini, K. Morimoto, T.O. Niinikoski, F. Udo, Dynamic polarization of protons, deuterons, and carbon-13 nuclei: thermal contact between nuclear spins and an electron spin-spin interaction reservoir. *J. Low. Temp.* **15**(3), 249–267 (1974)